

**SYNTHESIS OF GALLIUM NITRIDE (GaN)
NANOSTRUCTURES BY ELECTROCHEMICAL
TECHNIQUES FOR SENSING APPLICATIONS**

KHALLED MHAMMAD KALLEF AL-HEUSEEN

UNIVERSITI SAINS MALAYSIA

2011

**SYNTHESIS OF GALLIUM NITRIDE (GaN) NANOSTRUCTURES BY
ELECTROCHEMICAL TECHNIQUES FOR SENSING APPLICATIONS**

By

KHALLED MHAMMAD KALLEF AL-HEUSEEN

**Thesis submitted in fulfillment of the requirements
for the degree of
Doctor of Philosophy**

May 2011

ACKNOWLEDGMENTS

"All praises and thanks to ALLAH"

I would like to express my sincere appreciation and heartfelt thanks to my supervisor, Associate Professor Dr. Md. Roslan Hashim for his creative guidance, intellectual support, stimulating discussions and inspiring words. I am grateful for his excellent hospitality and wonderful attitude.

Great thanks for Universiti Sains Malaysia for providing me financial support for this research. Also, I would like to express my gratitude to the School of Physics, Universiti Sains Malaysia.

I would also like to express my appreciation to the staff in the Nano Optoelectronics Research Laboratory for their co-operation, technical assistance and valuable contribution to my work. The assistance from the staff of the Solid State Physics laboratory is also acknowledged.

Finally, words may not be sufficient to express acknowledgment to my family.

Khalled A-heuseen

Penang, Malaysia. May 2011

TABLE OF CONTENTS	Page
ACKNOWLEDGEMENTS	ii
TABLE OF CONTENTS	iii
LIST OF TABLES	ix
LIST OF FIGURES	x
LIST OF SYMBOLS	xv
LIST OF MAJOR ABBREVIATION	xvii
ABSTRAK	xviii
ABSTRACT	xx
CHAPTER 1 : INTRODUCTION	1
1.1 Fundamentals of III-V Nitrides and GaN	1
1.2 Overview and Background of Porous GaN	4
1.3 Overview and Background of GaN Growth Techniques	6
1.3.1 Hydride Vapor Phase Epitaxy (HVPE)	7
1.3.2 Metalorganic Chemical Vapour Deposition (MOCVD)	7
1.3.3 Molecular Beam Epitaxy (MBE)	8
1.3.4 Electrochemical Deposition Techniques	8
1.4 Overview of GaN-Based Sensors	11
1.4.1 Temperature-Dependant of Metal/GaN	11
1.4.2 Hydrogen Gas Sensor	13
1.4.3 Metal-Semiconductor-Metal Photodetectors	13
1.5 Research Objectives	14
1.6 Outline of the Thesis	15

CHAPTER 2: THEORY	16
2.1 Introduction	16
2.2 Principle of Photoelectrochemical Etching	16
2.2.1 Photoelectrochemical Etching Mechanism of GaN	17
2.3 Principles of Electrochemical Deposition	18
2.3.1 Faraday 's Law	19
2.3.2 Electrodeposition of Metal	20
2.3.3 Electrodeposition of Alloys	21
2.3.4 Electrodeposition of Semiconductors	21
2.3.5 Mechanism of Electrochemical Deposition of GaN	24
2.4 Theory of Metal-Semiconductor Contacts	25
2.4.1 Calculation of Barrier Heights and Ideality Factor	26
2.4.1.(a) Thermionic Emission Model	26
2.4.1.(b) Flat Band Barrier Height	28
2.4.1.(c) Current-Voltage-Temperature (I - V - T)	28
2.4.1.(d) Gaussian Modification of Richardson Plots	29
2.5 Fundamental of GaN-based Devices	31
2.5.1 Hydrogen Gas Sensor	31
2.5.1. (a) Gas Sensing Mechanism	31
2.5.1. (b) Sensitivity	32
2.5.1. (c) Response and Recovery Times	33
2.5.2 Metal-Semiconductor-Metal (MSM) Photodiode	33
2.5.2. (a) Quantum Efficiency	35
2.5.2. (b) Responsivity	35

2.5.2. (c) Response Time	35
CHAPTER 3: METHODOLOGY	37
3.1 Introduction	37
3.2 Methods for Metal Contacts	37
3.2.1 Wafer Cleaning	37
3.2.2 Metal Evaporation	38
3.2.3 Metal Sputtering	39
3.3 Method of Generating Porous GaN	40
3.3.1 Photoelectrochemical Etching Cell	40
3.3.2 Photoelectrochemical Etching Conditions	41
3.3.2. (a) Porous GaN using Different Current Density	41
3.3.2. (b) Porous GaN using Different Electrolytes	42
3.3.2. (c) Porous GaN using Different Durations	42
3.4 Method of Electrochemical Deposition of GaN	43
3.4.1 Preparation of Electrolytes	43
3.4.2 Preparing the Substrates	43
3.4.3 Electrochemical Deposition Cell	44
3.4.4 Synthesis Conditions of GaN using ECD Techniques	45
3.4.4. (a) Different Current Densities	46
3.4.4. (b) Different Durations	46
3.4.4. (c) Different Substrates	46
3.5 Method of Studying Metal/GaN Contacts	46
3.6 Fabrication and Characterization of Devices	47
3.6.1 Fabrication of Gas Sensor	47
3.6.2 Experimental Set Up and Characterization of Gas Sensor	48

3.6.3	Fabrication of M-S-M Photodiodes	48
3.6.4	Characterization of M-S-M Photodiodes	49
3.7	Instrumentations	49
3.7.1	Scanning Electron Microscopy (SEM) and Energy Dispersive X-Ray (EDX)	50
3.7.2	High Resolution X-Ray Diffraction (HR-XRD)	50
3.7.3	Photoluminescence (PL) and Raman Measurements	52
3.7.4	Hall Effect	53
3.7.5	Current-Voltage Measurements	53
CHAPTER 4: THE STUDY OF PHOTOELECTROCHEMICAL ETCHING OF GaN		54
4.1	Introduction	54
4.2	Photoelectrochemical Etching under Different Current Density	54
4.2.1	Surface Morphology	55
4.2.2	Photoluminescence(PL) Spectra	56
4.2.3	Raman Analysis	57
4.2.4	Optical Transmission	60
4.2.5	Temperature-Dependent of Metal-porous GaN contact	62
4.3	Effect of Different Electrolytes	69
4.3.1	Porosity and Surface Morphology	69
4.3.2	Photoluminescence (PL) Spectra	71
4.3.3	Raman Analysis	73
4.3.4	Electrical Properties of Electrolyte-GaN Junction	76
4.3.5	Metal–Semiconductor–Metal Ultraviolet Photodiodes	78
4.4	Electrochemical Formation of Porous GaN for Different Duration	81
4.4.1	Surface Morphology	81

4.4.2 J-t Characterization	83
4.4.3 Photoluminescence (PL) Spectra	84
4.4.4 Porosity Calculation	86
4.4.5 Raman Analysis	87
4.4.6 Hydrogen Gas Sensors Based on Schottky Barriers of Pd/ Porous GaN	89
4.5 Summary	95
CHAPTER 5: THE STUDY OF ELECTROCHEMICAL DEPOSITION OF GaN	97
5.1 Introduction	97
5.2 Synthesis of GaN Thin Films on Si (111) using Different Current Densities.	97
5.2.1 SEM and EDX of ECD GaN Films	97
5.2.2 X-Ray Studies of ECD GaN Films	99
5.2.3 Photoluminescence (PL) of ECD GaN Films	101
5.2.4 Raman Analysis of ECD GaN Films	102
5.2.5 Temperature-Dependent of Pd/ECD GaN Schottky Barrier Diodes	103
5.2.6 Thermal Annealing Effect on the Electrical Properties of Ni and Pd Contacts on ECD GaN/Si (111)	109
5.3 Synthesis of GaN Thin Films on Si Substrate for Different Durations	112
5.3.1 SEM and EDX of ECD GaN Films	112
5.3.2 XRD of ECD GaN Films	113
5.3.3 Photoluminescence(PL) of ECD GaN Films	116
5.3.4 Raman Analysis of ECD GaN Films	117
5.4 Synthesis of GaN Thin Films Deposited on Different Substrates	118
5.4.1 SEM and EDX of ECD GaN Thin Films	118

5.4.2 XRD of ECD GaN Films	119
5.4.3 Photoluminescence (PL) of ECD GaN Films	121
5.4.4 Raman Analysis of ECD GaN Films	122
5.4.5 Hydrogen Gas Sensors Based on Schottky Barriers of Ni/ECD GaN	123
5.4.6 Photodetectors Based on Schottky Barriers of Ni/ECD GaN	127
5.5 Summary	129
CHAPTER 6: CONCLUSIONS AND FUTURE DIRECTION	131
6.1 Conclusions	131
6.2 Future outlook	134
REFERENCES	135
Appendices	148
Appendix 1: Comparison Between the Properties of GaN, AlN and Si	148
Appendix 2: Schottky Contacts Formation	149
LIST OF PUBLICATIONS	153

	LIST OF TABLES	Page
Table 2.1	Electrical nature of Ideal MS Contacts.	26
Table 4.1	The peak positions, FWHM, peak shift and the relative intensity of near band edge PL of different samples.	57
Table 4.2	The phonon modes detected in the Raman spectra.	59
Table 4.3	The peak positions, FWHM, peak shift and the relative intensity of porous GaN etched using different electrolytes	72
Table 4.4	The phonon modes detected in the Raman spectra of porous GaN etched using different electrolytes.	75
Table 4.5	The photo-current measured at 4V, the series resistance, the Schottky barrier heights, and the ideality factors of different electrolytes-GaN contacts at room temperature	77
Table 4.6	The ideality factor, Schottky barrier height and dark and photo-current of as-grown and porous samples	79
Table 4.7	The phonon modes detected in the Raman spectra.	89
Table 5.1	Lattice parameters (a and c), in-plane strain (ϵ_a), out of plane strain (ϵ_c) and average crystal size determined for the GaN samples deposited for different current density.	100
Table 5.2	Ideality factor, barrier height, series resistance, built-in voltage and electron affinity for Pd/ECD GaN/Si (111) contact measured at different annealing temperatures.	111
Table 5.3	Ideality factor, barrier height, series resistance, built-in voltage and electron affinity for Ni/ECD GaN/Si (111) contact measured at different annealing temperatures.	111
Table 5.4	Lattice parameters (a and c), in-plane strain (ϵ_a), out of plane strain (ϵ_c) and average crystal size determined for the h-GaN samples deposited for different durations.	116
Table 5.5	The ideality factor, SBH, dark and photo-current of the two diodes	128

	LIST OF FIGURES	Page
Figure 1.1	Wurtzite crystal structure of GaN (Maruska and Tietjen, 1969).	3
Figure 1.2	Road map of electrodeposition of main inorganic semiconductors (Lincot, 2005). Grey areas correspond to research intensity. MS: molten salts; AQ: aqueous solvent; NAQ: non-aqueous solvent; ECALE: Electrochemical Atomic Layer Electrodeposition. Numbers in bold letters are years, numbers in italic letters are temperatures in °C.	10
Figure 2.1	The MSM structure used in the fabrication of MSM photodiode	34
Figure 3.1	Image of the thermal evaporator.	38
Figure 3.2	Image of the RF sputtering equipment in the lab.	39
Figure 3.3	The photoelectrochemical etching experimental set up used to generate porous GaN.	41
Figure 3.4	Schematic drawing of the first type of a conventional electrochemical deposition cell, where the Ga plates was used as an anode and the Si as a cathode.	44
Figure 3.5	Schematic drawing of the second type of a conventional electrochemical deposition cell, where the metallic gallium kept in glass tube and capped at the end with a sintered glass diaphragm was used as an anode and the Si as a cathode.	45
Figure 3.6	The schematic diagram of hydrogen gas sensing system	48
Figure 3.7	The MSM structure used in the fabrication of MSM photodiode in this thesis	49
Figure 3.8	Scanning electron microscope (SEM) for high magnification optical observation, energy dispersive X-ray (EDX) and electron beam lithography (EBL).	50
Figure 3.9	Image of high resolution XRD equipments.	51
Figure 4.1	SEM images of porous GaN samples prepared with different etching current densities; a) 5 mA/cm ² , b) 10 mA/cm ² , and c) 20 mA/cm ² , and d) the etching rate with current density.	55
Figure 4.2	Photoluminescence spectra of porous GaN etched with different current densities: (a) as-grown, (b) 5 mA/cm ² , (c) 10 mA/cm ² and (d) 20 mA/cm ² .	56

Figure 4.3	Raman spectra of samples etched with different current densities; as-grown GaN, 5 mA/cm ² , 10 mA/cm ² and 20 mA/cm ² , indicated by (a), (b), (c) and (d) respectively: (A) for the range from 100-200 cm ⁻¹ and (B) for the range from 500-800 cm ⁻¹ .	58
Figure 4.4	Raman spectra showing the small shift of E ₂ (high) for porous samples (samples b, c and d) compared to that of as-grown (sample a).	60
Figure 4.5	Optical transmission spectra of porous GaN etched with different current densities and as-grown.	61
Figure 4.6	Temperature dependent <i>I-V</i> logarithmic plot for the; (a) as-grown and (b) porous Pd/GaN Schottky diode in the temperature range (300-470K).	62
Figure 4.7	The variation of ideality factor and barrier heights as a function of temperature for as-grown and porous samples Pd/GaN Schottky diodes.	64
Figure 4.8	The flat barrier height for as-grown and porous Pd/n-GaN Schottky diodes versus temperature.	64
Figure 4.9	The variation of series resistance as a function of temperature for as-grown and porous samples Pd/GaN Schottky diodes.	65
Figure 4.10	Richardson plot, $\ln(I_0/AT^2)$ versus $1/(kT)$ for the two diodes as-grown and porous Pd/GaN in the temperature range 300-470K.	66
Figure 4.11	Zero-bias apparent barrier height and ideality factor versus $q/(2kT)$ curves of the as-grown and porous Pd/GaN Schottky diodes according to the Gaussian distribution of the barrier heights.	68
Figure 4.12	Modified Richardson plot for the Pd/GaN Schottky diodes for the two samples, as-grown and porous, according to the Gaussian distribution of barrier heights.	68
Figure 4.13	SEM images of samples etched under different electrolytes a) HF: C ₂ H ₅ OH, b) HF: HNO ₃ , c) KOH and d) H ₂ SO ₄ : H ₂ O ₂ .	70
Figure 4.14	PL Intensity of samples etched under different electrolytes a) as-grown b) HF: C ₂ H ₅ OH, c) HF: HNO ₃ , d) KOH and e) H ₂ SO ₄ : H ₂ O ₂ .	71
Figure 4.15	The Raman spectra of samples etched under different electrolytes (A) and the small shift of E ₂ (high) for porous samples	74

Figure 4.16	Characteristics of the different electrolytes/GaN at room temperature in linear scale and logarithmic scale.	77
Figure 4.17	<i>I-V</i> characteristics of the fabricated as-grown and porous Ni/GaN/Ni MSM photodiodes measured in dark (dark current) and under UV illumination (photocurrent), the inset is the gain.	78
Figure 4.18	Measured spectral responsivities at room temperature and voltage 5V of the as-grown and porous Ni/GaN/Ni photodetectors.	80
Figure 4.19	Scanning electron microscopy images of porous GaN samples prepared under different etching duration: (a) 10 min, (b) 15 min, (c) 20 min, and (d) 30 min.	82
Figure 4.20	Current density versus time during GaN electrochemical etching process.	83
Figure 4.21	Photoluminescence spectra of porous GaN etched under different durations: (a) 10 min, (b) 15 min, (c) 20 min, (d) 30 min, and (e) as-grown. Inset shows photoluminescence for the range between 390 and 490 nm.	85
Figure 4.22	Variation of porosity with etching time based on (a) equation 4.5 (b) equation 4.1.	87
Figure 4.23	Raman spectra of GaN samples etched under different duration: (a) 10 min, (b) 15 min, (c) 20 min, d) 30 min, and (e) as-grown.	88
Figure 4.24	The (<i>I-V</i>) characteristics at room temperature of (a) Pd/as-grown GaN and (b) Pd/porous GaN gas sensors as a function of hydrogen flow rate.	90
Figure 4.25	The series resistances at room temperature of Pd/as-grown GaN (inset) and Pd/porous GaN as a function of hydrogen flow rate.	91
Figure 4.26	(a) The barrier height (ϕ_b) and (b) the ideality factor (n) of Pd/as-grown GaN and Pd/porous GaN gas sensors as a function of hydrogen flow rate.	92
Figure 4.27	Sensitivity of the Pd/as-grown GaN and Pd/porous GaN gas sensors as a function of hydrogen flow rate at voltage 3V.	93
Figure 4.28	The on-off currents of the porous GaN gas sensors operating at room temperature for a constant voltage of 1V exposed to different hydrogen flow rates.	94
Figure 5.1	SEM images and EDX spectra of GaN thin films deposited by different current densities, (a) 1.5, (b) 2.5, (c) 3.5 and (d) 4.5 mA/cm ² .	98

Figure 5.2	XRD of deposited GaN films on Si (111) using different current densities of 1.5, 2.5 and 3.5mA/cm ² indicated by a, b and c respectively for 12hrs, (A) for the range of $2\theta=25-45^\circ$, (B) for the range of $2\theta=58.5-59.5^\circ$	99
Figure 5.3	PL spectra of deposited GaN films on Si (111) for 12h using different current densities; (a) 1.5, (b) 2.5, and (c) 3.5mA/cm ² .	101
Figure 5.4	Raman spectra of GaN deposited on Si (111) for 12h and current density 2.5 mA/cm ² .	103
Figure 5.5	(a) Temperature dependent <i>I-V</i> plot of the Pd/GaN Schottky diode in the temperature range (300-470K) and (b) series resistance versus operating temperature.	105
Figure 5.6	Barrier heights and ideality factors as a function of temperature in the temperature range (300-470K) for the as-deposited Pd/GaN Schottky diode.	105
Figure 5.7	Richardson plot, $\ln (I_0/AT^2)$ versus $1/(kT)$, in the temperature range (300–470K) for the Pd/ECD GaN Schottky diode.	107
Figure 5.8	Ideality factor (a) and apparent barrier height (b) versus $q/(2kT)$ curves of the Pd/ECD GaN/Si(111) Schottky diode according to the Gaussian distribution of the barrier heights.	108
Figure 5.9	Modified Richardson plot for the Pd/ECD GaN/Si (111) Schottky diode according to the Gaussian distribution of barrier heights.	109
Figure 5.10	<i>I-V</i> characterization of the metal/ ECD GaN/Si (111) at different annealing temperatures for (a) Pd and (b) Ni.	110
Figure 5.11	Barrier height and ideality factor as a function of annealing temperature for (a) Pd and (b) Ni/ECD GaN/Si (111) Schottky diode.	111
Figure 5.12	Scanning electron microscopy images and EDX spectrum of the four GaN films deposited under different duration: (a) 6 h, (b) 12 h, (c) 24h, and (d) 48h.	113
Figure 5.13	A) XRD of the four GaN films deposited under different durations: (a) 6 h, (b) 12 h, (c) 24 h, and (d) 48 h and B) peak intensity of h-GaN and c-GaN versus deposition time	114
Figure 5.14	(A) Variation of lattice constants (<i>a</i>) and (<i>c</i>) and grain size <i>D</i> of h-GaN with different deposition time and (B) Variation of film thickness with different deposition time and the variation of lattice parameters with film thickness .	115

Figure 5.15	PL spectra of the four GaN films deposited under different duration: (a) 6 h, (b) 12 h, (c) 24 h, and (d) 48 h.	117
Figure 5.16	Raman spectra of the four GaN films deposited under different duration: (a) 6 h, (b) 12 h, (c) 24 h, and (d) 48 h.	118
Figure 5.17	SEM images and EDX spectra of GaN thin films deposited by constant current density 2.5 mA/cm^2 for 12h on different substrates (a) Si (111), (b) Si (100) and (c) ITO coating glass.	119
Figure 5.18	XRD of deposited GaN on different substrates; (a) Si (111), (b) Si (100) and (c) ITO.	121
Figure 5.19	PL spectra of deposited GaN for 12 h using constant current density 2.5 mA/cm^2 on three substrates; (a) Si(111), (b) Si(100), and (c) ITO.	121
Figure 5.20	Raman spectrum of deposited GaN for 12 h using constant current density 12.5 mA/cm^2 on three substrates; (a) Si(111), (b) Si(100), and (c) ITO.	122
Figure 5.21	(<i>I-V</i>) curves of Ni/GaN/MSM gas sensors measured at room temperature for different hydrogen flow rate for two samples (a) ECD GaN/ Si (111) and (b) ECD GaN/Si (100).	124
Figure 5.22	Variation of (a) barrier potential (ϕ_b) and (b) ideality factor (n), with different H_2 flow rate for MSM gas sensors of Ni/ECD GaN Schottky diode on Si (111) and Si (100).	124
Figure 5.23	Sensitivity as a function of hydrogen flow for MSM gas sensors of Ni/ECD GaN on Si (111 and Si (100) at room temperature.	126
Figure 5.24	Response behavior of representative MSM gas sensors of Ni/ECD GaN on Si (111 and Si (100) at 2V.	127
Figure 5.25	<i>I-V</i> characteristics of the fabricated Si (111) and Si (100) Ni/ECD GaN/Ni MSM photodiodes measured in dark (dark current) and under UV illumination (photocurrent) and the gain in the inset.	128
Figure 5.26	Measured spectral responsivity at room temperature and voltage 3.5V of the ECD GaN/Si (111) and ECD GaN/Si (100) MSM photodetectors.	129

LIST OF SYMBOLS

a	Lattice constant
A	Area
A^{**}	Richardson's constant
c	Lattice constant
d	Interplanar spacing of the crystal planes
D	Average crystal size
e	Charge of electron
E_C	Conduction band
E_F	Fermi level of semiconductor
E_g	Semiconductor band gap
E_v	Valence band edge
(hkl)	Miller indices
I	Current
I_o	Saturation current
J	Current density
k	Boltzmann constant
m_o	Electron mass
m^*	Effective mass
m_n	Electron effective mass
m_p	Hole effective mass
N_C	Effective density of states
N_D	Donor concentration
N_A	Acceptor concentration
N_i	Number of sites (dipole moment) per area at the interface
n	ideality factor
n	Free electron concentration
p	Free hole concentration
P	Porosity
q	Electron charge
R	Responsivity
R	Resistance
R_H	Hall coefficient
R_c	Contact resistance
R_s	Series resistance
S	Sensitivity
T	Thickness
t	Time
T	Absolute temperature
V	Volume
V	Voltage
V_d	Diffusion voltage
V_H	Hall voltage
ΔV	Electrical polarization
w	Width
W_C	Width of the pad
W_D	Depletion layer width
α	Absorption coefficient
ε_a	Strain along a-axis

ε_c	Strain along c-axis
ε_o	Absolute dielectric constant
ε_r	Relative dielectric constant
σ	Conductivity
σ_s	Standard deviation
ν	Frequency
θ_i	Hydrogen atoms coverage at the interface
θ	Incident / Diffraction angle
χ	Semiconductor electron affinity
φ_B	Schottky barrier height
φ_{BF}	Flat band barrier height
ϕ_M	Metal work function
ϕ_S	Semiconductor work function
μ_n	Electron mobility
μ_p	Hole mobility
μ	Effective dipole moment
ρ	Resistivity
∞	Infinity
ω	Photon frequency
λ	Wavelength
η	Quantum efficiency
β	Contrast ratio of photo and dark current

LIST OF MAJOR ABBREVIATIONS

a.u.	Arbitrary unit
BL	Blue luminescence
CB	Conduction band
DAP	Donor-acceptor pair
DBE	Donor bound exciton
DC	Direct current
ECD	Electrochemical deposition
EDX	Energy Dispersive X-ray
eV	Electron volt
FE	Field Emission
FWHM	Full width at half maximum
HEMT	High Electron Mobility Transistor
HVPE	Hydride vapor phase epitaxy
I-V	Current-Voltage
LD	Laser Diode
LED	Light Emitting Diode
LO	Longitudinal optic
M	Metal
MBE	Molecular Beam Epitaxial
MESFET	Metal-Semiconductor FET
MOCVD	Metalorganic vapor deposition
MOSFET	Metal-Oxide-Semiconductor FET
MS	Metal Semiconductor
MSM	Metal Semiconductor Metal
O.T	Optical transmission
PC	Photocurrent
PGaN	Porous GaN
PECE	Photoelectrochemical etching
PL	Photoluminescence
RL	Red luminescence
RMS	Root mean square
SBH	Schottky barrier height
SC	Semiconductor
sccm	Standard cubic centimeters per minute
SEM	Scanning electron microscope
TEM	Transmission electron microscopy
TFE	Thermionic field emission
TLM	Transmission line model
TO	Transverse optic
UHV	Ultra high vacuum
UV	Ultra Violet
VB	Valence-band
XRD	X-ray Diffraction
YL	Yellow luminescence
WZ	Wurtzite structure
ZB	Zinc blend structure

SINTESIS STRUKTUR NANO GALLIUM NITRIDE (GaN) MELALUI TEKNIK ELEKTROKIMIA UNTUK APLIKASI PENDERIAAN

ABSTRAK

Tujuan utama kerja penyelidikan ini adalah untuk membina struktur nano GaN menggunakan dua teknik elektrokimia kos rendah iaitu punaran fotoelektrokimia (PECE) dan endapan elektrokimia (ECD). Dalam kategori pertama kerja ini, GaN berliang telah dihasilkan menggunakan teknik fotoelektrokimia (PECE) dalam beberapa keadaan seperti ketumpatan arus, kadar masa dan elektrolit yang berbeza. Keputusan kajian menunjukkan bahawa saiz liang secara purata adalah sensitif terhadap ketumpatan arus, dan elektrolit yang berbeza pula yang menghasilkan morfologi yang berbeza. Spektrum Raman dari semua sampel berliang dengan puncak E_2 (tinggi) menunjukkan bahawa relaksasi stres telah terjadi di semua sampel. Mekanisme PECE keatas GaN telah diteliti, dan dua model punaran untuk PEC GaN mencadangkan bahawa lapisan oksida terbentuk pada permukaan GaN di bawah UV dan kemudian larut dalam elektrolit.

Dalam kategori kedua, filem nipis GaN dibuat dengan teknik (ECD) menggunakan larutan nitrat dengan mencampurkan galium ($\text{Ga}(\text{NO}_3)_3$) dengan nitrat amonium (NH_4NO_3) ke dalam air yang diionisasi. Ion-ion positif Ga^{+3} dan NH_3^{+1} tertumpu pada permukaan katod. Kombinasi dari kedua-dua ion positif telah membentuk kluster saiz kritikal GaN. Kesan dari parameter endapan yang berbeza juga boleh mempengaruhi kualiti GaN juga telah dikaji iaitu ketumpatan arus, masa endapan dan substrat yang berbeza. Filem-filem GaN mengandungi fasa campuran h-GaN dan c-GaN dengan saiz butiran di sekitar 18-29 nm.

Dalam projek ini, dua peranti telah difabrikasi iaitu pengesan gas hidrogen dan pengesan cahaya MSM. Diod Schottky berasaskan Pd/GaN berliang

mempamerkan perubahan dramatik arus setelah terdedah ke gas hidrogen dibandingkan dengan diod Schottky Pd/GaN hablur tunggal. Didapati bahawa prestasi pengesan cahaya pada GaN berliang jauh lebih baik daripada GaN hablur tunggal. Nisbah arus foto kepada arus gelap (β) pada 3V untuk sampel berliang dan hablur tunggal adalah masing-masing 1241 dan 78. Selain itu, prestasi dua peranti, iaitu pengesan gas hidrogen dan MSM juga telah dikaji keatas endapan Ni pada ECD GaN/Si (111) dan ECD GaN/Si (100). Ketinggian sawar diukur dan didapati meningkatkan dengan kadar aliran hidrogen, dan jelas bahawa ECD GaN pada Si (111) lebih sensitif daripada GaN pada Si (100). Pengukuran menunjukkan bahawa sensitiviti pengesan cahaya MSM dibuat pada ECD GaN / Si (111) lebih baik dari ECD GaN / Si (100) dan nilai (β) pada 3.5V masing-masing adalah 52 dan 14.

SYNTHESIS OF GALLIUM NITRIDE (GaN) NANOSTRUCTURES BY ELECTROCHEMICAL TECHNIQUES FOR SENSING APPLICATIONS

ABSTRACT

The main goal of this work presented in this thesis was to fabricate nanostructures of GaN using two low-cost electrochemical techniques namely photoelectrochemical etching (PECE) and electrochemical deposition (ECD). In the first category of this work, the porous GaN was generated using photoelectrochemical etching techniques under different conditions, i.e. current density, different duration of etching and different electrolytes. The results showed that the average pore size was sensitive to the current density, and different electrolytes generated different morphology. The Raman spectra of all porous samples with E_2 (high) peak suggested that stress relaxation has taken place in all samples. The mechanism of PECE etching of GaN was investigated, and a two-step etching model for PEC of GaN proposed that an oxide layer was formed on the GaN surface under UV and then dissolved in the electrolyte.

In the second category, GaN thin films were synthesized by a low-cost ECD technique using an aqueous solution prepared by mixing gallium nitrate ($\text{Ga}(\text{NO}_3)_3$) with ammonium nitrate (NH_4NO_3) in deionized water. The positive ions of Ga^{+3} and NH_3^{+1} were concentrated on the surface of the cathode. Combination of these two positive ions formed clusters of critical sizes of GaN. The effects of different parameters that may affect the quality of the deposited GaN were studied. GaN films contained mixed phases of h-GaN and c-GaN with grain sizes in the range of 18-29 nm.

In this work, two devices were fabricated, hydrogen gas sensors and MSM photodetectors. The Pd/porous GaN Schottky diode exhibited a dramatic change of

current after the exposure to hydrogen gas as compared to the Pd/as grown GaN Schottky diode. It was found that the performance of the UV- photodetector on porous GaN was more sensitive than that on as-grown. The contrast ratio of photocurrent and dark current (β) at 3V for porous sample and as-grown was found to be 1241 and 78, respectively. Two devices, i.e. hydrogen gas sensors and MSM were also fabricated by depositing Ni on ECD GaN/Si (111) and on ECD GaN/Si (100). The barrier height measured was found to be increased with hydrogen flow rate, and it was clear that the ECD GaN on Si (111) had better response than ECD GaN on Si (100). Measurements revealed that the sensitivity of the MSM photodetector fabricated on ECD GaN/Si (111) was better than that on ECD GaN/Si (100) and the β at 3.5V was 52 and 14 for the two photodetectors, respectively.

CHAPTER 1

INTRODUCTION

1.1 Fundamentals of III-V Nitrides and GaN

Nowadays, information technology is mainly based on semiconductors electronics. In particular, in the last decades computers and their networks allowed a huge development of our society in several areas, like telecommunication, transportation, etc. In fact, the rapid progress of semiconductors electronics could meet the strong demand of technology.

For several years silicon-based devices have been further developed and to date have represented the core of the entire semiconductor industry. However, the recent developments have reached the theoretical limit of silicon, such as temperature (150 °C) and breakdown voltage (300V) limits, thus leading to the need of using other semiconductors with properties that cannot be reached by using silicon.

Recently, the III-V nitrides namely GaN, AlN, InN and their alloys have received much attention because of their promising semiconductor device applications in the electronics as well as optoelectronics operating in the blue and ultraviolet (UV) region of the light spectrum. The focus on the III-V nitrides has been motivated by the lack of semiconductor materials satisfying commercial demands for blue, green, and UV lasers and light-emitting devices in previous years. The wavelength range of these continuous alloy systems formed by the nitrides with direct band gaps spans from 1.9 eV for InN, 3.4 eV for GaN, to 6.2 eV for AlN thus, covering the technologically important UV and visible spectral ranges (Strite and Morkoc, 1992)

Among all the III-V nitrides, GaN is considerably the most intensely studied. GaN is a direct and wide band gap semiconductor. With its superior radiation hardness and chemical stability, together with its large band gap characteristic, these properties have made GaN a suitable semiconductor material for device applications in the high-temperature and caustic environment as well as in space applications. GaN is also an attractive candidate for protective coatings due to its radiation hardness (Strite and Morkoc, 1992). Its wide band gap makes it goes intrinsic to a much higher temperature than materials like Ge, Si and GaAs that is the intrinsic carrier concentration at any given temperature decreases exponentially with band gap, and therefore, GaN is attractive for high temperature applications.

Moreover, due to its many attractive features like higher sheet charge densities, higher mobilities, better charge confinement, and higher breakdown voltages, GaN is also a potential candidate for the application in electronic devices such as at high temperature, high power and for high frequency transistors (Razeghi and Rogalski, 1996; Ali and Gupta, 1991; Sze, 1990). The transparency of high quality GaN at wavelengths longer than the band gap makes it an ideal material for fabricating photodetectors capable of rejecting near infrared and visible regions of the solar spectrum while retaining near unity quantum efficiency in the UV. Besides, in optoelectronics, GaN is primarily of interest for its potential as a blue and UV light emitter (Strite and Morkoc, 1992).

Many properties of semiconductors are determined by their crystalline structure. The common crystal structure of group III-Nitrides and GaN is wurtzite. Although the rock-salt or zinc-blende structure is possible depending on growth conditions and the type of substrates, the wurtzite form P_{63mc} (C46v) is thermodynamically stable in ambient environment. The rock-salt structure is a

structure transformed from wurtzite at high external pressure. The zinc-blende structure is metastable and may be stabilized by epitaxial growth on Si, GaAs, MgO and 3H SiC. However, the majority of research has been focused on the wurtzite crystal phase, since the growth of the wurzite structure is easier and cheaper than that of the cubic one. Indeed, the hexagonal structure is stable and can be grown on various substrates like sapphire, SiC and Si (Guha and Bojarczuk, 1998; Lei et al., 1993).

Figure 1.1 illustrates the wurtzite structure. In this figure, the Ga atoms are represented by black beads while the N atoms are represented by white beads. The wurtzite lattice is characterized by two parameters: the edge length of the base hexagon ($a = 3.189 \text{ \AA}$) and the height of the hexagonal lattice cell ($c = 5.185 \text{ \AA}$) (Maruska and Tietjen, 1969).

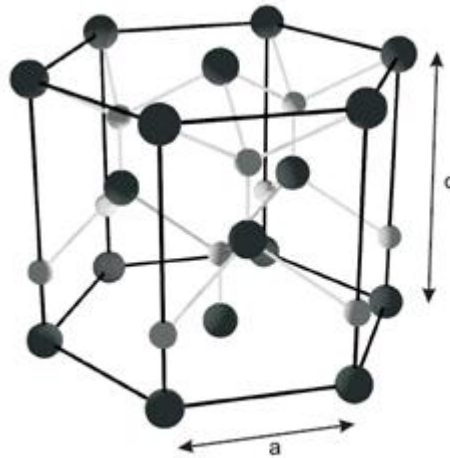


Figure 1.1: Wurtzite crystal structure of GaN (Maruska and Tietjen, 1969).

The most important physical properties of GaN, for both wurtzite and zinc blend, significant for electronic devices, are reported and compared with those of Si and AlN in the table in Appendix 1. As example, it presents a high band gap and a high critical electric field material. Due to the strong ionic component of the bond

between the Ga atom and the nitrogen atom, the GaN is highly stable structurally and chemically. Hence, GaN is a highly stable compound even at elevated temperatures. It has bond energy of 8.92 eV/atom. GaN also, displays superior resistance to most chemicals and of conventional wet etchants is known to etch in hot KOH solution only. In fact, this chemical stability combined with its hardness makes GaN an attractive material for protective coating.

1.2 Overview and Background of Porous GaN

The synthesis of nanostructure materials is a key to their practical applications and has attracted much attention in the last decade. Many techniques have been developed to synthesize nanostructure materials, such as electrochemical etching (porous). During the last decades, nanocrystalline semiconductors have been widely studied because of their particular physical and chemical properties and perspectives for applications. A cheap, three-dimensional processing and simple technology of photoelectrochemical etching is one of the most versatile techniques for fabrication of nanocrystalline or porous materials. Formation of pores during anodization process has been widely reported for various types of crystalline silicon. The compound semiconductors such as GaAs (Oskam et al., 1997), GaN (Yam et al., 2007; Guo et al., 2006; Vaipheyi et al., 2005), InP (Tsuchiya et al., 2003) and GaP (Elhoichet et al., 2005) have been investigated in the form of porous layers.

Recently, many works (Shaoqiang et al., 2005; Beji et al., 2003; Missaoui et al., 2002; Montes et al., 2000; Dhar and Chakrabarti, 2000;) have been directed towards depositing semiconductor layers on porous substrates, because of the demand for more powerful and sophisticated device applications. One of the reasons for using a porous semiconductor as a substrate for depositing semiconductor layers

is that the nano-patterned porous structure would lead to a reduced extended defect density (Beji et al., 2003). The interest in porous semiconductor arises from the fact that it can act as sink for threading dislocations and accommodate the strain. Hence, it is widely used as a buffer or intermediate layer in epitaxial growth so as to obtain a subsequent layer with lowered strain and dislocation density (Qhalid Fareed et al., 2004; Mynbaeva et al., 1999). Mynbaeva et al. (2000) proposed that the growth of GaN on porous GaN can lead to high-quality strain-released epilayers.

For formation and processing of GaN nanostructures, two main methods were used; metal-assisted electroless chemical etching, and photo-assisted electrochemical etching. The former attracts attention of many researchers, because it does not need electrical contact substrates, but this approach lacks the control of the pores size and size distribution. The later however, possess unique features such as low process temperature, low process damage, process simplicity, versatility and low processing costs. Thus, for certain applications, it may become a viable low-damage and low-cost alternative to the main-stream approach based on the conventional semiconductor technology (Alifragis et al., 2005). In this method, the applied voltage and current, electrolyte composition, and illumination conditions control etch rate and, thus, morphology, and optical properties. This approach requires a conducting substrate which is robust to the optimum electrochemical etching conditions (Diaz et al., 2003). However, one can unravel this problem by using front contact instead of back contact (Al-heuseen et al., 2011; Al-heuseen et al., 2010). Several researchers have used this method at high power UV light up to 500 W to illuminate the GaN surface, hence the dominant parameter effected the etching process was the UV light, resulting in reduction of the effect of the applied current (Risti et al., 2003; Skriniarova et al., 2001).

1.3 Overview and Background of GaN Growth Techniques

Producing and fabricating high quality electronics devices like LEDs, LDs, photo detectors etc, requires growing of high quality GaN doped thin films. Selecting appropriate substrate to deposit the film on is one of the main factors that affect GaN growth techniques. The most common substrates used to grow GaN are; sapphire (Al_2O_3), SiC and Si substrates. For each one of these substrates there are many advantages and disadvantages briefly mentioned next. The first is sapphire (Al_2O_3) which is an interesting choice because it is a semi-insulating, high growth temperature and it is relatively cheap, but it has some disadvantage to grow GaN, it has a large lattice mismatch (13%) (Popovici and Morkok, 2000), large thermal expansion coefficient mismatch (34%) and low thermal conductivity. These reasons make it the worst choice for high-power application. The second choice is SiC substrate which is better than sapphire for microwave high-power application, because it is low lattice mismatch (3.4%) (Torvik and Pankove, 2000), low thermal expansion coefficient mismatch (25%) and high thermal conductivity, but its bad choice for light application because it is not UV-transparent. The third choice is Si substrate with advantages, such as low cost, excellent availability of large substrate dimension and acceptable value of thermal conductivity, but it still has large thermal expansion coefficient mismatch (56%) and large lattice mismatch (17%) (Tansley et al., 1997).

In recent years, many efforts have been made to grow GaN thin films by various conventional growth techniques, including metalorganic chemical vapor deposition (MOCVD) (Amano et al., 1994), molecular beam epitaxy (MBE) (Nikishin et al., 1999), hydride vapour phase epitaxy (HVPE) (Jasinski et al., 2001),

reactive sputtering (Nahlah et al., 1998) and electrochemical deposition (Al-Heuseen et al., 2010). In this section, we present a brief of some of these techniques.

1.3.1 Hydride Vapor Phase Epitaxy (HVPE)

In the early investigation of GaN, HVPE was the most successful epitaxial growth technique to grow GaN thin films which was developed by Maruska and Tietjen (1969). In their method, HCl vapor flowing over a Ga melt, cause the formation of GaCl which was transported downstream. At the substrate, GaCl mixed with NH₃. The early GaN grown by this technique had very high background n-type carrier density, typically $\sim 10^{19} \text{cm}^{-3}$ (Pankove, 1973).

1.3.2 Metalorganic Chemical Vapour Depositions (MOCVD)

Generally, chemical vapour deposition or CVD is a process in which high quality thin layers of intrinsic or doped layers of semiconductors can be grown. The substrate is heated to high temperatures where chemical decomposition, called pyrolysis of a gas, generally takes place directly on the surface of the heated substrate.

For GaN growth, MOCVD reactors incorporate laminar flow at high operating pressures and feature separate inlets for the nitride precursors and the ammonia to minimize predeposition reactions. Suitable precursors should be used such as those possessing good reactivity, thorough pyrolysis, and transportability. Preferably, the precursors should be nonpyrophoric, water and oxygen insensitive, noncorrosive, and nontoxic. Trimethylgallium (TMG) and triethylgallium (TEG) are very popular for Ga, though GaCl has been tried. Ammonia (NH₃) is considered the best source of nitrogen, as it is reasonably pure and stable.

1.3.3 Molecular Beam Epitaxy (MBE)

Molecular beam epitaxy can be dated back to the year 1958 when Gunther (Gunther et al., 1958) described a technique of growing compounds on heated substrate by evaporation from two sources. The major developments towards modern MBE equipment were made by Cho and Arthur in 1975 (Cho et al., 1975). The growth chamber is the heart of an MBE system. During the growth process, elemental sources are heated in Knudsen cells and evaporated at controlled rate onto a heated substrate under ultra-high vacuum (UHV) conditions $\sim 10^{-10} - 10^{-11}$ Torr. The UHV growth environment is crucial to the MBE process. It provides an ultra clean growth ambient leading to epitaxial layers with the highest purity. This is extremely important for growing high quality semiconductor materials which are used for high performance devices. Under UHV condition, the long mean-free path of particles minimizes collisions or reactions between molecules in the beam, which results in a line-sight growth reaction at the surface. GaN films growth by MBE are usually carried out at relatively low temperatures of 650 - 800 °C with typical growth rate of one to three monolayers per second, approximately 0.3 to 1 $\mu\text{m/h}$.

1.3.4 Electrochemical Deposition Techniques

Electrochemical deposition is a fascinating phenomenon, that one can put a coating of one material on another simply by donating electrons to ions in a solution and the studies of the process at an atomic level continue to yield surprises. Electrochemical deposition is exceptionally versatile, and many valuable applications keep being invented (Izaki and Omi, 1996). Comparing to other techniques, the advantages of the electrochemical deposition (ECD) are as follows: the thickness and surface morphology can be controlled by growth parameters, the deposition rate is

relatively high, the experimental setup is low-cost, it is a low temperature process, and ECD makes the doping of the impurities easy (Katayama and Izaki, 2000; Gu and Fahidy, 1999; Izaki and Omi, 1996).

Electrochemical deposition (ECD), which has been widely used for metal or metallic alloys, was used recently for semiconductors. Electrochemical deposition of semiconducting materials thus represents a new challenge, not only from the academic point of view, but also from the economic point of view, since this method presents interesting characteristics for large area of semiconductors, low cost and generally low temperature and soft processing of materials. However, the application of the electrochemical deposition technique to semiconductors has been limited until recently, mainly because of complexities in the electrodeposition of semiconductors and the stringent materials property requirements for device applications. Research and development in the area of semiconductor electrodeposition have been continued after the pioneering work by Kröger in (1978) and Panicker et al. (1978). They found that both n- and p-type polycrystalline CdTe layers could be produced by cathodic electrodeposition using acidic sulfate electrolytes containing Cd^{2+} and HTeO^{2+} ions. Afterwards, other semiconductor compounds such as CuInSe_2 and CuInS_2 has been synthesized by electrodeposition techniques (Oliveria et al., 2002; Pottier and Maurin, 1989; Mishra and Rajeshwar, 1989).

Many research groups have extensively investigated and studied the electrodeposition of the compound semiconductors. Bhattacharya (1983) was the first one who reported on synthesis CuInSe_2 by ECD. Chandra and Khare (1987) performed the electrodeposition of GaAs from an acidic bath. De Mattei et al. (1978) carried out the electrodeposition of GaP from a solution containing sodium metaphosphate, NaF, and Ga_2O_3 . Electrochemical preparation of thin films of ZnTe

was first reported by Basol and Kapur using two-stage process involving electrodeposition of Te and Zn stacked layers from aqueous electrolytes followed by annealing (Basol and Kapur, 1988). Electrochemical deposition of ZnO has initially been introduced by Pauporte and Lincot (1999) and Izaki et al. (1996) using GaN and ITO substrates, respectively. In figure 1.2, Daniel Lincot put a road map of the electrochemical deposition of main inorganic semiconductors.

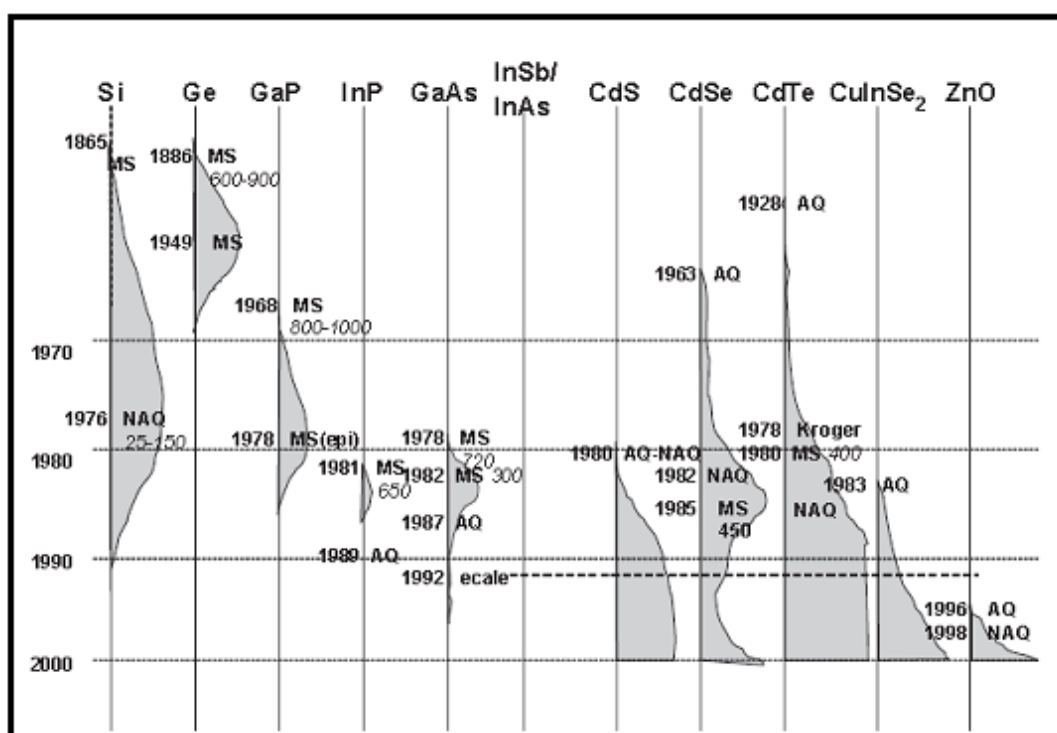


Figure 1.2: Road map of electrodeposition of main inorganic semiconductors (Lincot, 2005). Grey areas correspond to research intensity. MS: molten salts; AQ: aqueous solvent; NAQ: non-aqueous solvent; ECALE: Electrochemical Atomic Layer Electrodeposition. Numbers in bold letters are years, numbers in italic letters are temperatures in °C

Figure 1.2 also indicates the onset of an impetuous development of the electrodeposition of oxides, led by ZnO, which was introduced in 1996 (Peulond and Lincot, 1996). Electrodeposition appears very well suited for oxides; most of them are semiconducting materials. These compounds are also highly ionic which is expected to be a favorable criterion.

Electrochemical deposition of GaN is still in the beginning. Reports on using ECD to grow GaN thin film are limited. Roy and Pal (2005) were the first who reported the synthesis of GaN films using electrodeposition technique. They used a constant current density and potential above room temperature where Si (100) and ITO was used as a substrate. In this work we synthesis GaN thin film using a simple and low-cost electrochemical deposition on n-Si (111) substrates and for the first time below room temperature at 20 °C with different current densities (Al-heuseen et al., 2010). In a few years it is hopefully expected that a great interest in this approach would take place by many researchers for its cheapness and ease and thus, it is anticipated that the quality of GaN films deposited by this technique would be enhanced.

1.4 Overview of GaN-Based Sensors

The interest in GaN and related materials has been increased in recent years due to their prosperous future as the base materials for fabricating the optoelectronic devices and high power, high temperature electronic devices such as gas sensor and photodetectors. Metallic contacts to GaN films are an essential part of most modern electronic and optoelectronic devices. The electronic structure of metal/GaN interfaces at different temperatures plays a fundamental role in the transport properties of these junctions.

1.4.1 Temperature-Dependant of Metal/GaN

To construct high quality GaN-devices, it is necessary first to clarify the physics of metal/GaN interface and its influence on electrical characteristics of metal/GaN Schottky diodes. Many researchers have used high work function metals

as Schottky contacts like Ni, Pt and Pd on GaN (Tan et al., 2006; Rajagopal, 2005; Deba et al., 2002; Liu et al., 1997; Binari et al., 1997). It is well known that the electrical characteristics of a Schottky contact are controlled mainly by its interface properties. Thus, the study of interface states is important for the understanding of the electrical properties of Schottky contacts.

The analysis of the I - V characteristics of metal/semiconductor diodes at wide temperature range allows us to understand different aspects of barrier formation and current-transport mechanisms and gives information about the quality of the contacts especially at temperatures higher than room temperature. A lot of works have already been reported on electrical characterization but there are few works by which the temperature dependence of electrical characteristics of GaN Schottky diodes are being studied. Akkal et al. (2004) investigated the current-voltage characteristics of Au/n-GaN Schottky diodes below room temperature in the range 80-300 K. Osvald et al. (2005) investigated the temperature dependence of the electrical characteristics of GaN Schottky diodes with two crystal polarities (Ga- and N-face). They reported a decrease in the barrier height with decreasing temperature and an increase in ideality factor for both polarities. Arehart et al. (2006) studied the impact of threading dislocation density on the Ni/n-GaN Schottky diode using forward measurements. Tekeli et al. (2007) investigated the behavior of the forward bias (I - V - T) characteristics of inhomogeneous (Ni/Au) - $\text{Al}_{0.3}\text{Ga}_{0.7}\text{N}/\text{AlN}/\text{GaN}$ heterostructures in the temperature range of 295-415 K using double layers of metal and multi layers of GaN and AlN. Recently, Ravinandan et al. (2009) reported on the temperature-dependent electrical characteristics of the Au/Pd/n-GaN Schottky diode in the temperature range of 90-410 K.

1.4.2 Hydrogen Gas Sensor

Hydrogen is one of the most important applied gases, and there are significant recent interests in the development of hydrogen gas sensors for use in fuel cells as an energy source to replace petroleum. Hydrogen gas sensors play a critical role, particularly for fuel leak detection in spacecraft, automobiles, and aircraft, fire detectors, and diagnosis of exhaust and emissions from industrial processes since hydrogen is a hazardous, odorless, and highly flammable gas (Dobrokhoto et al., 2006; Voss et al., 2005; Steinhoff et al., 2003; Connolly et al., 2002). Hydrogen sensors that are capable to operate in harsh environmental conditions such as high temperature and chemically corrosive ambient are highly desirable. GaN is the ideal material for that, due to its wide-bandgap and thermal stability. The material is also chemically stable, with the only known wet etchant being molten NaOH or KOH, making it very suitable for operation in chemically harsh environments or in radiation fluxes. In addition, GaN gas sensors have the unique advantage of integration with GaN-based solar-blind UV photodetector or high power, high temperature electronics units on the same chip.

1.4.3 Metal-Semiconductor-Metal Photodetectors

Detection of ultraviolet (UV) radiation is an important feature for many applications such as environmental, military, and industrial fields, for instance: flame monitor, water purification system, money counting, photochemical phenomena detection, etc. (Razeghi et al., 1996). In recent years, many researchers have been focusing on semiconductor-based ultraviolet (UV) photodiodes and gallium nitride (GaN) is one of the most promising materials for the fabrication of high-responsivity and visible-blind UV detectors, since it has a large direct bandgap energy (3.41 eV at

room temperature) and a high saturation electron drift velocity (310 cm/s) (Pankove, 1990). The superior radiation hardness and high temperature resistance of GaN also make it the suitable material for UV detectors working in extreme conditions (Biyikli et al., 2004; Pau et al., 2004).

In the past few years, various types of GaN-based photodetectors have been proposed, such as p-n junction diode (Monroy et al., 1998), p-i-n diode (Parish et al., 1999), p- π -n diode (Osinsky et al., 1997), Schottky barrier detector (Chen et al., 1997), and metal-semiconductor-metal (MSM) photodetector (Huang et al., 1997). Among these, MSM photodetectors exhibit superior performance in terms of the response speed, device noise, and fabrication simplicity. To achieve a large Schottky barrier height on GaN, one can choose metals with high work functions such as gold (Au), platinum (Pt), palladium (Pd), and nickel (Ni).

1.5 Research Objectives

The principal objectives of this project can be summarized in the following points:

1. To fabricate and to study the porous GaN constructed using photoelectrochemical etching under different conditions.
2. To synthesis GaN nanostructures using low cost electrochemical deposition techniques under different conditions.
3. To study the electrical properties of Ni and Pd metal on GaN films at different temperatures. These metallization schemes will be used in the fabrication of different devices.
4. To study the synthesized films as gas sensors and photodetectors.

1.6 Outline of the Thesis

The outline of the thesis is as follows: Chapter 1 deals with a literature overview of the research on GaN etching and deposition and the main properties of these materials. The general principles and theories of the electrochemical deposition principles and mechanism of GaN, metal-semiconductor contact, porous GaN formation mechanisms as well as the basic principles of some devices (which have been fabricated in this thesis) are covered in Chapter 2. In Chapter 3, the methodology and instrumentation involved in this thesis are described.

The results obtained from the research works are analyzed and discussed in Chapters 4 and 5. Chapter 4 focuses on the study of the properties and applications of the porous GaN using photoelectrochemical etching. Chapter 5 presents the experimental results of the electrochemical deposition of GaN thin films and their properties synthesized under different parameters. Finally, Chapter 6 presents the conclusions of our work and suggestions for the future.

CHAPTER 2

THEORY

2.1 Introduction

General principles and theories of all subjects involved in this work are presented in this chapter. It starts with a brief explanation of the principles of photoelectrochemical etching. The fundamental of electrochemical deposition principles and the mechanism of GaN formation and the fundamental theories for metal-semiconductor contacts are also addressed. Furthermore, the basic principles of some devices, which have been fabricated in this research, which are gas sensor and metal-semiconductor-metal (MSM) photodetector, are briefly described in this chapter.

2.2 Principles of Photoelectrochemical Etching

Photoelectrochemical (PEC) etching is a technique encompassing light-induced generation of electrons and holes assisting electrochemical reactions of semiconductors in contact with an electrolyte. When immersed in an electrolyte, the semiconductor exchanges electrons with the electrolyte along the surface because the Fermi level in the semiconductor is different from that of the electrolyte. Like semiconductor-metal contacts, an energy barrier is formed, the effective height of which is often fixed by the distribution of surface states in the semiconductor. At the same time, a source of light whose photon energy is greater than the bandgap energy of the semiconductor illuminates the semiconductor surface, resulting in pairs of electrons and holes being photogenerated. The electrons and holes created in the space-charge region near the surface are transported by two mechanisms, drift under

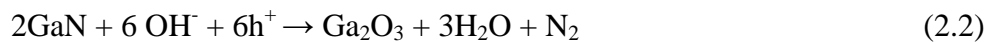
the influence of the electric field, and diffusion due to the carrier concentration gradient.

2.2.1 Photoelectrochemical Etching Mechanism of GaN

When a GaN sample is immersed into the electrolyte, the GaN electrode-electrolyte interface energy band diagram resembles a semiconductor-metal interface. Thus a Schottky contact is formed. When a reverse bias is applied to the n-GaN surface, the energy band bends in the downward direction, and a potential well for holes is formed and this depleted the electrons from the GaN surface. If the sample is illuminated by photon energies above GaN bandgap at 300 K, electron-hole pairs are generated in the semiconductor. The electrons and holes created in the space-charge region near the surface are transported by two mechanisms; drift under the influence of the electric field, and diffusion due to the carrier concentration gradient. The swept photogenerated holes are confined at the electrolyte/semiconductor interface due to the band bending (Seo et al., 1993). It has been accepted by many researchers that the following reaction equations are responsible for the PEC etching of GaN (Trichas et al., 2008; Goncalves et al., 2007; Zhuang and Edgar, 2005; Rotter et al., 2000; Rotter et al., 1998)



A two-step model can describe the photoelectrochemical-etching process. At first, an oxide layer is formed on the GaN surface, governed by equation:



Then, the oxide layer is dissolved in the electrolyte:



Both holes and OH^- ions take active parts in the etching of the GaN. It should be noted that the two-step process described by Eqs. (2.2) and (2.3) is essentially equivalent to the overall reaction described by Eq. 2.1. It has been observed that bubbles are often found near the surface of the sample during PEC etching, which may come from the release of N_2 . In addition, the photoelectrochemical etching current decreased gradually due to the increasing oxide thickness. During the chemical etching, bond exchange proceeds simultaneously between undissociated molecules and the surface atoms in the solution. Chemical bonds between the surface atoms and the bulk atoms are broken while new bonds are formed between Ga and O_2 and move to the solution.

2.3 Principles of Electrochemical Deposition

Electrochemical Deposition is a process where the metallic ions become solid metal and are deposited on the cathode surface when a sufficient amount of electric current passes through an electrolyte or plating solution that contains charged ions. These charged ions, especially positively charged ions, can be produced by dissolving metallic salt in water. Electrochemical Deposition is exceptionally versatile, and valuable applications keep being invented. The advantages of the electrochemical deposition (ECD) in comparison with other methods are as follows: the thickness and surface morphology can be controlled by growth parameters, the deposition rate is relatively high, the experimental setup is low-cost, it is a low temperature process, and ECD makes the doping of the impurities easy (Katayama and Izaki, 2000; Gu and Fahidy, 1999; Izaki and Omi, 1996). Historically electrochemical deposition was limited to metal deposition, commonly known as electroplating. As the understanding of electrochemistry increased with time, more

complex materials such as metal alloys, metal compounds and semiconducting materials deposition procedures have been developed. The deposition is carried out in an electrochemical cell consisting of a reaction vessel and two or three electrodes. In the two-electrode cell, the reactions are controlled by the current applied between a working electrode (substrate) and a counter electrode. In the three-electrode cell a reference electrode is used to control or measure the potential of the working electrode, and deposition is carried out by controlling either current or potential and the corresponding potential or current, respectively, may be measured.

2.3.1 Faraday's Law

Faraday's law states that the amount of electrochemical reaction that occurs at an electrode is proportional to the quantity of electric charge Q passed through an electrochemical cell. From this law we get (Endres et al., 2008)

$$m = \frac{1}{nF} \int I dt \quad (2.4)$$

and the thickness (T) of the deposition layer can be calculated from the following equation :

$$T = \frac{w}{AD} = \frac{M}{nFAD} \int I dt \quad (2.5)$$

where m is the number of reduced moles, n is the number of electrons taking part in the reduction, I is the current, t is the deposition time, w is the weight of the deposit, A is the electrode area, D is the density of the deposited material, F is the Faraday constant and M is the atomic/molecular weight of the deposit. Since the thickness of deposition depends on the current passing through the electrolyte during a certain

time interval, it is possible to measure the thickness of deposition simply by measuring the current.

2.3.2 Electrodeposition of Metals

Electroplating of metals is a very mature technique. It has a very wide variety of applications. In relation to solar cells there are several possible applications such as; deposition of front or back contacts of solar cells, deposition of reflective back contact for thin film solar cells.

The theory of electroplating is based on the positively charged, conductivity and reactions of the plating metals and electrons. It can be explained in a simple formula (Endres et al., 2008)



In the formula above, M stands for the plating metal (the M charge changes with each type of metal), and n equals to the number of electrons needed to cancel the charge. These combined to make the final metal coating or M^0 .

The plating of metals mainly depends on the physical properties and composition of the metal that is going to be plated. Some may not be good conductors, thereby making poor cathodes for the electroplating process. Others may not plate well because of a strength-weight ratio of the metal to be plated. If the strength to weight ratio is low, then the plating material may not hold well with the metal. If the strength to weight is high, then the plating will hold well to the metal, ensuring a good bond between the two.

Anodes are probably one of the most important things to consider in electroplating. The anodes work better if they are made up of an alloy that also contains the plating metal. This helps ensure that proper positive ions of the plating metal are

conducted through the electrolyte. Finally the studying of metal deposition is the first step to understand the deposition of alloys and semiconductors compounds.

2.3.3 Electrodeposition of Alloys

The electrodeposition of an alloy requires, by definition, the co-deposition of two or more metals. In other words, their ions must be present in an electrolyte that provides a cathode film, where the individual deposition potentials can be approximately same. This is achieved by changing the concentration of ions in the solution which changes the activity of reaction in Eq. 2.6.

2.3.4 Electrodeposition of Semiconductors

The electrodeposition of semiconductors is emerging as a simple method for the fabrication of thin films and nanostructure for use in optoelectronic and photovoltaic applications. Thin films of semiconductors used in optoelectronic application are usually fabricated from the vapour phase or liquid phase. Vapour depositions such as physical vapour (Coevaporation, molecular beam epitaxy), and chemical vapour deposition (CVD) are the most common ways to fabricate these materials.

Liquid phase deposition includes crystallization from the molten phase or aqueous phase for instance liquid phase epitaxy (LPE). For all of the above techniques, there are a lot of physical and chemical conditions that must be applied in order to obtain a high quality thin film applicable in optoelectronic devices as electroluminescence or laser diodes, photo detectors or high efficiency photovoltaic devices. For instance deposition temperatures higher than room temperature are generally used in the routine methods of fabrication.

Although electrochemical deposition of metals have been used for several years but this method in particular has been almost completely absent from the area of semiconductors. However, recently chemical bath deposition (CBD) and electrodeposition (ED) of semiconductors have emerged as competitive techniques for growth of high quality thin films for applications in sensitive detectors.

Electrodeposition bath for coating semiconductor materials are very similar to that one in growth of metals. Here the substrate on which the thin film is going to grow, is considering as a working electrode (WE) and connected to the negative pole of power supply. The positive pole must be connected to an inner metal which does not affect the deposition, such as platinum. In electrochemical bath this electrode is called secondary electrode (SE) which is the anode electrode. Due to the potential control between electrolyte (solution) and WE another electrode is used, and this electrode which is called the reference electrode (RE) plays an important role for applying a fix potential on the surface of working electrode which is independent to the applied current between SE and WE.

Electrodeposition is a very sensitive method which can be affected by several factors during thin film growth. For fabricating a high quality thin film surface all of these factors must be optimized. These factors are temperature, pH, ion concentration, effective voltage, current density and etc. The pH of electrolyte is dependent on the concentration of Hydrogen ions in the solution which can be calculated by $\text{pH} = -\log [\text{H}^+]$, and can be controlled by some buffer solution like NaOH or H_2SO_4 . Temperature also plays an important role in growth of high quality thin films because some materials cannot be coated at room temperature thus, this factor must be optimized for each material. Solidification of ions takes place in the solution near to cathode electrode starting from dissolved precursors (mostly in ionic

form), the electrodeposition of semiconductors can proceed cathodically or anodically. The reaction should be preceded when the applied potential is lower than the redox potential of the reaction for cathodic process. When compound semiconductors are to be deposited, the solution should include all the ions for all elements in a soluble form.

In general, the electrodeposition of semiconductor compounds, like any other chemical process, is governed by thermodynamic considerations. In the case of electrodeposition, the reactions are thermodynamically unfavorable; that is, the overall free energy change (ΔG) for the reaction is positive because the deposition will be on negative substrate. The electrical energy supplies the needed energy to drive the reaction. Consider, the case of an ion M^{+n} as in equation 2.3 being reduced to M, then the change in free energy is given by (Paunovic, et al., 2006)

$$\Delta G = \Delta G^0 + RT \ln \left[\frac{a_M}{a_{M^{+n}}} \right] \quad (2.7)$$

where R is the gas constant, T is the absolute temperature and a_M is the activity of species M. In the solution case, activity is related to the concentration by the activity coefficient $a = \gamma [M^{+m}]$. Then Eq. 2.7 becomes

$$\Delta G = \Delta G^0 + RT \ln \left[\frac{1}{M^{+m}} \right] \quad (2.8)$$

It can be shown that

$$\Delta G = -nFE \quad (2.9)$$

where n is the number of moles of electrons involved in the reaction, F is Faraday's constant and E is the potential. Equation 2.8 may now be written:

$$E = E_0 - \frac{RT}{nF} \ln \frac{1}{[M^{+m}]} \quad (2.10)$$

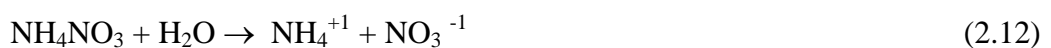
where E_0 is the standard electrode potential for reaction (Eq. 2.6) referenced to the standard electrode with $[M^{+m}] = 1$ mole/liter. Equation 2.10 is called Nernst equation and it becomes more complicated for compound semiconductors.

2.3.5 Mechanism of Electrochemical Deposition of GaN

Electrochemical deposition of GaN is still in the beginning. There are limited numbers of reports about using ECD in GaN thin films. Roy et al. (2005) was the first to report the synthesis of GaN films using electrodeposition technique. They used constant current density and potential for depositing GaN on Si substrate above room temperature. We have grown GaN thin film using a simple and low-cost electrochemical deposition on n-Si (111) substrates and for the first time below room temperature at 20°C with different current densities (Al-heuseen et al., 2010).

GaN thin films were prepared by electrochemical technique using an aqueous solution, which was prepared by mixing gallium nitrate ($Ga(NO_3)_3$) with ammonium nitrate (NH_4NO_3) in a ratio of (1:1) in deionized water kept at 20 °C since Ga metal melts at 29 °C (Al-Heuseen et al., 2010; Roy et al., 2005). N-type Si (111) was used as a substrate. The possible mechanism of electrochemical deposition of GaN thin films may be as follows:

When gallium nitrate and ammonium nitrate dissolved in water, the possible reactions that take place in the cell can be written as:



The positive ions of Ga^{+3} and NH_3 were concentrated on the surface of cathode (Si substrate). Combination of these two positive ions will form clusters of critical sizes of GaN as in Eq. 2.14. In addition, the formation of NH_3 is the key of the GaN formation reaction because this compound reacts with gallium nitrite to produce the GaN thin films, all possible reaction occurs in the high concentration of NH_4^+ . The first step of this reaction is the formation of small clusters of critical sizes which subsequently lead to growth of continuous films on the surface of Si.

2.4 Theory of Metal-Semiconductor Contacts

The metal-semiconductor contact forms an important link between the semiconductor and the outside world. Thus, a contact simply is referred to as the region of metal semiconductor interface that leads to desirable electrical characteristic. The current transport in metal-semiconductor contact occurs by majority carriers. There are two different types of contacts namely ohmic and Schottky. In ohmic contact, the current-voltage relation follows Ohms law that is it should be linear. The resistance of contact should be very low so that there is negligible voltage drop across it and hence negligible power drop. The other type of contact is Schottky contact, or rectifying contact in which large current can flow in one direction at small voltage and almost no current in reverse direction. High barrier height is essential for producing rectifying effects.

Whether a metal-semiconductor interface forms an ohmic or Schottky contact depends upon the metal work function, ϕ_m , and semiconductor work function, ϕ_s . Work function is the amount of energy required to excite an electron from Fermi energy level to the vacuum level. Theoretically, on n-type semiconductor, ohmic contact is formed when $\phi_m < \phi_s$ and Schottky contact is formed when $\phi_m > \phi_s$.